Small-angle x-ray-scattering study of phase separation and crystallization in the bulk amorphous $Mg_{62}Cu_{25}Y_{10}Li_3$ alloy

W. Liu* and W. L. Johnson
W. M. Keck Laboratory of Engineering Materials, 138-78, California Institute of Technology, Pasadena, California 91125

S. Schneider and U. Geyer
I. Physikalisches Institut and Sonderforschungsbereich 345, Universität Göttingen, D-37073 Göttingen, Germany

P. Thiyagarajan†
Intense Pulsed Neutron Source Division, Argonne National Laboratory, 9700 South Cass Avenue, Argonne, Illinois 60439
(Received 30 November 1998)

We report on a small-angle x-ray-scattering (SAXS) and differential scanning calorimetry study of phase separation and crystallization in rapidly quenched amorphous $Mg_{62}Cu_{25}Y_{10}Li_3$ alloy samples. Differential scanning calorimetry demonstrates the occurrence of crystallization and grain growth upon isothermal annealing of these samples at 135 °C. The SAXS studies show the presence of large inhomogeneities even in the rapidly quenched as-prepared $Mg_{62}Cu_{25}Y_{10}Li_3$ alloy that is attributed to phase separation in the undercooled liquid during the cooling process. After isothermal annealing at 135 °C for longer than 30 min the samples exhibit a strong SAXS intensity that monotonically increases with increasing annealing time. During heat treatment, crystallization and growth of a nanocrystalline bcc-Mg_7Li_3 phase occurs in the Y-poor and MgLi-rich domains. The initially rough boundaries of the nanocrystals become sharper with increasing annealing time. Anomalous small-angle x-ray-scattering investigations near the Cu *K* edge indicate that while Cu is distributed homogeneously in the as-prepared sample, a Cu composition gradient develops between the matrix and the bcc-Mg_7Li_3 nanocrystals in the annealed sample. [S0163-1829(99)01018-8]

I. INTRODUCTION

The new family of bulk metallic glasses[1] offers excellent opportunities for studying the glass transition and properties of the supercooled liquid state of metallic systems. In addition, crystallization mechanisms can be delineated in great detail in these systems. In a number of multicomponent metallic-glass-forming systems such as La-Al-Ni,[2] Zr-Y-Ni-Al,[3] and Zr-Ti-Cu-Ni-Be,[4–6] phase separation in the amorphous or supercooled liquid states has been observed and identified to be closely related to the primary crystallization process. Studies of phase separation therefore become important in understanding the thermal stability and the crystallization processes in metallic glasses.

Mg-Cu-Y is known to be a good bulk metallic glass that can form fully amorphous rods with a diameter up to 7 mm.[7,8] Previous studies on bulk samples prepared at cooling rates of about 10^3 K/s revealed that the addition of a small amount of Li results in a microstructure consisting of a high density of nanocrystals embedded in a phase-separated amorphous matrix.[9] In this paper, we present small-angle x-ray-scattering (SAXS) and differential scanning calorimetry (DSC) investigations on phase separation and primary crystallization in rapidly quenched $Mg_{62}Cu_{25}Y_{10}Li_3$ foils prepared at a cooling rate of approximately 10^6 K/s.

II. EXPERIMENT

$Mg_{62}Cu_{25}Y_{10}Li_3$ alloys were prepared by induction melting a mixture of the elements of purity ranging from 99.9% to 99.999% on a water-cooled silver boat under a Ti-gettered argon atmosphere. The ingots were repeatedly remelted to ensure homogeneity. Then, small pieces of samples were levitation-melted in a high-frequency coil and quenched into thin foils in a twin-piston splat quencher under clean Ar atmosphere at a cooling rate of about 10^6 K/s.[10] The average thickness of the foils is about 50 μm. DSC measurements were carried out by using a Perkin-Elmer differential scanning calorimeter. For the SAXS measurements, disks with a diameter of 3 mm were cut from splat-quenched samples. These disks were annealed in the glass transition region at 135 °C for different times. After heat treatment, the samples were analyzed by wide-angle x-ray diffraction using a Phillips diffractometer. The SAXS measurements were done at the SAXS beamline BL 4-2 at the Stanford Synchrotron Radiation Laboratory.[11] The elastically scattered x-rays (wavelength 1.5 Å) were measured by using a 20-cm-long position-sensitive gas detector at a sample-to-detector distance of 2.3 m. This provided data in a Q range of 0.008–0.12 $Å^{-1}$ [$Q=(4\pi/\lambda)\sin\theta$, where λ is the wavelength of the x rays and 2θ is the scattering angle]. The incident and transmitted beam intensities were continuously monitored by two ion chambers on either side of the sample. The measured SAXS data were properly corrected for the incident beam intensity, transmission factor, the thickness of the sample, and the variation in the detector sensitivity across the detector. Such normalization is essential for comparing the anomalous small-angle x-ray-scattering (ASAXS) data[12–14] measured at different energies. Although the data were not placed on an absolute intensity scale, the scattering data of all samples were measured in the same instrument configuration and thus can be meaningfully compared. Prior to the

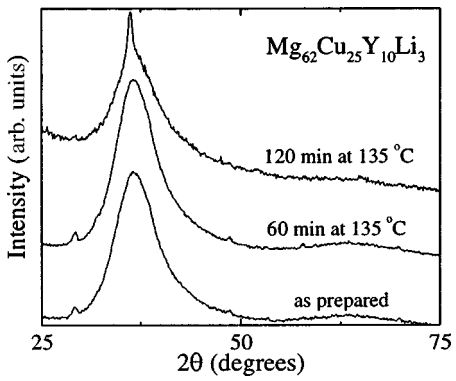

FIG. 1. X-ray diffraction patterns of the splat-quenched $Mg_{62}Cu_{25}Y_{10}Li_3$ in the as-prepared state and after annealing for 60 and 120 min at 135 °C.

ASAXS measurements we had determined the x-ray absorption edge of Cu in the same beam line by measuring the x-ray absorption spectra for a standard copper foil and one of our samples. The absorption edges for these differed by less than 1 eV.

III. RESULTS AND DISCUSSION

Figure 1 shows wide-angle x-ray diffraction patterns of a splat-quenched as-prepared $Mg_{62}Cu_{25}Y_{10}Li_3$ sample and isothermally annealed samples for 60 and 120 min at 135 °C. These data suggest that the as-prepared sample and the one annealed for 60 min are mainly amorphous. Our previous transmission electron microscopy (TEM) studies[9] of the as-prepared bulk samples showed small nanocrystals of about 20–40 Å diameter embedded in an amorphous matrix, but the volume fraction of these nanocrystals was so small that x-ray diffraction did not detect this nanophase. However, the diffraction pattern of the sample annealed for 120 min exhibited a crystalline peak corresponding to the bcc-Mg_7Li_3 phase.[9] Differential scanning calorimetry data for the as-prepared and isothermally annealed $Mg_{62}Cu_{25}Y_{10}Li_3$ samples at 135 °C for 60 and 120 min are shown in Fig. 2. For the as-prepared sample, the onset of the glass transition temperature at a heating rate of 40 K/min is 133 °C and the primary crystallization starts at 177 °C corresponding to the formation and growth of the bcc-Mg_7Li_3 phase.[15] The width of the undercooled liquid region decreases, the primary crystallization signal broadens, and its magnitude decreases with annealing time. The second exothermic peak near 200 °C is due to the crystallization of the remaining amorphous matrix into the intermetallic Mg_2Cu phase[9] and shifts to a lower temperature after heat treatment.

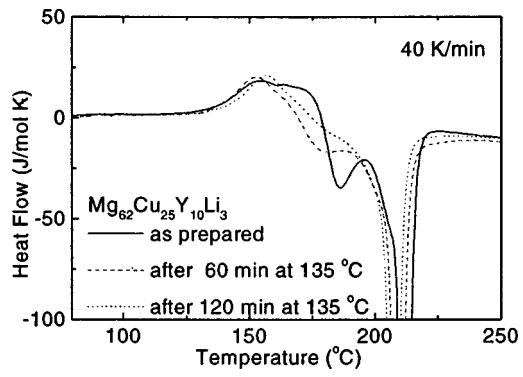

FIG. 2. DSC scans for $Mg_{62}Cu_{25}Y_{10}Li_3$ samples heat treated for different times at 135 °C at a heating rate of 40 K/min.

Small-angle x-ray scattering provides information on the size, shape, and concentration of inhomogeneities on a length scale up to tens of nm.[16,17] In cases where the interparticle distance is much larger than the particle size (dilute regime) SAXS data will yield the true particle size. However, for complex systems with dominating interparticle interactions, the size, molecular weight, and number density obtained from the SAXS data may be slightly different from those of a dilute system.[16]

Our analysis of the small-angle x-ray scattering data of the $Mg_{62}Cu_{25}Y_{10}Li_3$ samples is based on Eq. (1) and the curve fitting package in IGOR Pro.[18] This analysis allows us to obtain information on the radius of gyration of the inhomogeneities (from the exponential regime of the data) and on their interfacial properties (from the power-law regime of the data):[19]

$$I(Q)=I(0)\exp\left(-\frac{Q^2R_g^2}{3}\right)+B\left[\frac{\left[\operatorname{erf}\left(\frac{QR_g}{\sqrt{6}}\right)\right]^3}{Q}\right]^p. \quad (1)$$

In Eq. (1), R_g is the radius of gyration, i.e., the root-mean-squared distance of all the atoms from the center of the scattering volume, the prefactor $I(0)$ is the extrapolated intensity at $Q=0$ (discussed later), p is the power-law exponent, and B is the prefactor specific to the type of power-law scattering specified by the regime in which the exponent p falls. In the case of samples containing particles of constant scattering length density distributed in a matrix (two-phase system), Porod's law states that the power-law exponent for a sharp interface should have a value of $p=4$ and the prefactor $B=2\pi(\Delta\rho)^2S$.[17] Here, $\Delta\rho$ is the difference in the electron densities of the particles and the matrix (scattering contrast) and S is the surface area of the scattering interface. Many complex systems exhibit scattering behavior resulting from fractal topology.[20] The fractal nature of the system can be delineated from the power-law exponents derived from the scattering data.[21–23] If $I(Q)$ varies as Q^{-p} in a Q region, where $QR_g \gg 1$, then $p<3$ denotes that the scattering system may be a mass fractal[22,23] and $3<p<4$ corresponds to a surface fractal.[21] The fractal dimension of the surface, D_s, is $D_s=6-p$.[21] The extent of deviation of p from 4 can be used as a qualitative measure of the surface roughness. The prefactor $I(0)=NV^2(\Delta\rho)^2$,[24] where N is the number of particles per unit volume, V is the volume of the particle, and $\Delta\rho$ is the difference in the electron density between the particles and the matrix. The increase in the value of $I(0)$ with annealing can be qualitatively used as a measure of the growth of the particle size. Nonlinear curve fitting of the SAXS data in a wide Q region by using Eq. (1) was done to obtain the R_g, power-law exponents, and appropriate prefactors. The experimental data were weighted by the standard deviation at each Q.

Figure 3 shows the SAXS data of the as-prepared sample as well as of that annealed for 30 min at 135 °C. The SAXS data of the as-prepared sample exhibit a power law of $p=3.3$ in the $0.008<Q<0.03$ Å^{-1} region. This implies that

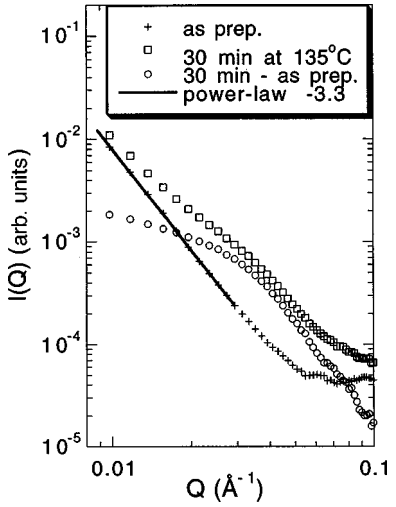

FIG. 3. The SAXS data of an as-prepared $Mg_{62}Cu_{25}Y_{10}Li_3$ sample, a sample annealed at 135 °C for 30 min, and the difference between the annealed sample and the as-prepared sample. The as-prepared sample exhibits power-law scattering from a surface fractal.

the as-prepared splat-quenched sample already consists of large phase-separated domains in accordance with Ref. 9. The average size of these inhomogeneities is larger than 20 nm and their interfaces exhibit a considerable roughness. The SAXS intensity of the annealed $Mg_{62}Cu_{25}Y_{10}Li_3$ samples at 135 °C is higher than that for the as-prepared sample and the SAXS intensity increases further with increasing annealing duration. As we will discuss below, this excess intensity is related to the formation and growth of nanocrystals in one of the phase-separated domains. Assuming that the decomposition into two amorphous phases occurs only during the cooling process at much higher temperatures than 135 °C, we have subtracted the scattering intensity of the as-prepared sample from the data for the sample annealed for 30 min. As shown in Fig. 3, the subtracted data for the annealed sample contain both an exponential and a power-law regime. Thus the radius of gyration $I(0)$ and the surface roughness of the nanocrystals can be readily derived.

Similarly, we have subtracted the SAXS data for the as-prepared sample from all other data sets. These subtracted data were fitted by using Eq. (1). Figure 4 shows the experimental data and the fits, respectively. Table I collects R_g, $I(0)$, and p values for all the annealed samples.

The results in Table I show that the R_g monotonically increase with increasing annealing time from 58 Å after 30 min to 94 Å after 120 min. Subsequent annealing up to 240 min causes only a minimal increase in the R_g value to 95 Å. This suggests that a constraint exists that prevents the crystals to grow beyond a finite maximum size. Table I also contains $I(0)$ values derived from the fits for samples annealed at various times. While R_g saturates after 120 min of annealing, the corresponding $I(0)$ values show a significant increase upon further annealing. This could be related to the growth of smaller crystals that evolve later as $I(0)$ is proportional to the V^2 of the particles.

The power-law exponent from the SAXS data of the annealed samples provides information on the surface roughness of the nanocrystals. The p values obtained from fitting

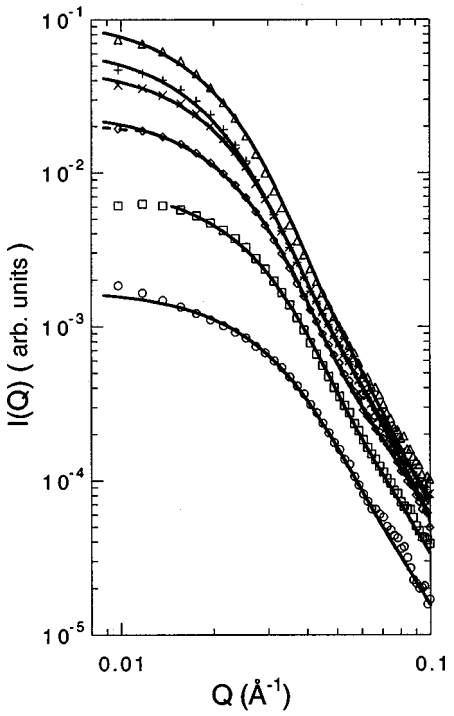

FIG. 4. The SAXS data of $Mg_{62}Cu_{25}Y_{10}Li_3$ samples, annealed at 135 °C for 30 min (○), 45 min (□), 60 min (◇), 90 min (×), 120 min (+), and 240 min (△) after the subtraction of the data for the as-prepared sample. The lines are the fits obtained by using Eq. (1), which provided the values for R_g and the power-law exponents.

of the SAXS data of the samples annealed at 135 °C at $0.05 < Q < 0.1$ Å^{-1} remain about 3.3 during the initial stages of annealing up to 60 min (Table I). With further annealing p increases and reaches a limiting value of 4 after 240 min. This power-law scattering behavior with annealing implies that the nanocrystals exhibit fractal surface topology in the initial stages of their growth. Upon further annealing the nanocrystals develop sharp interfaces, possibly to reduce their surface energy.

Anomalous small-angle x-ray scattering is an extension of SAXS experiments in which the energy of the probing x rays is varied near the absorption edge of an element in the sample.[12–14] By performing SAXS experiments with x-ray energies close to the characteristic absorption edges of a given atom, it is possible to vary the contrast for scattering of that particular element. The ASAXS data were collected at 8776, 8940, 8960, 8969, and 8973 eV (close to the Cu K edge at 8979 eV) with an energy resolution of $\Delta E \approx 2$ eV at each energy. Figure 5 shows the ASAXS data for the

TABLE I. Parameters obtained from the fitting of the SAXS data of $Mg_{62}Cu_{25}Y_{10}Li_3$ samples annealed for various times.

Sample	R_g (Å)	$I(0)$ (a.u.)	p
30 min	58±1	0.002	3.31±0.2
45 min	68±1	0.008	3.29±0.1
60 min	79±1	0.025	3.29±0.1
90 min	87±1	0.050	3.44±0.1
120 min	94±1	0.068	3.79±0.1
240 min	95±1	0.111	4.00±0.2

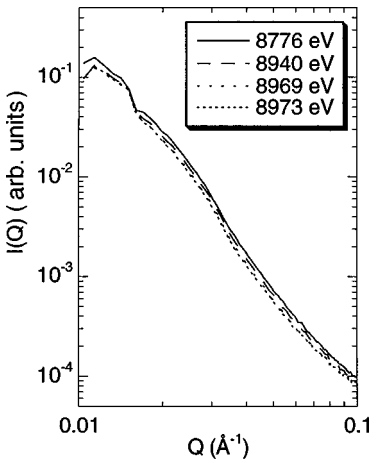

FIG. 5. The ASAXS near the Cu absorption edge (8979 eV) of $Mg_{62}Cu_{25}Y_{10}Li_3$ after annealing for 120 min at 135 °C.

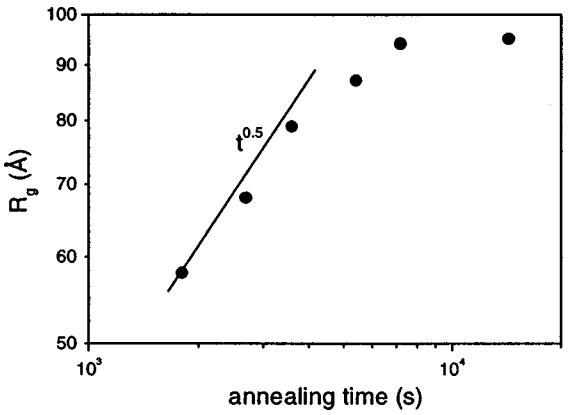

FIG. 6. The apparent radius of gyration R_g as a function of annealing time.

$Mg_{62}Cu_{25}Y_{10}Li_3$ sample annealed for 120 min at 135 °C. The error bars due to counting statistics are smaller than the size of the symbols. The scattering intensity at a given Q monotonically decreases as the energy of the probing x rays increases towards the absorption edge. ASAXS data measured for the as-prepared sample under identical conditions did not exhibit any such variation, implying that Cu is not involved in the phase separation. Our previous TEM results[9] have shown Mg-Li–rich and Mg-Li–poor domains. Since Cu is not involved in phase separation we conclude that the Mg-Li–rich domains are Y poor. It is known that for the Mg-Y-Cu system the thermal stability of the amorphous phase decreases with decreasing Y concentration.[7,8] Thus, the formation of nanocrystals is expected in these Y-poor domains. During crystallization, a Cu composition gradient develops between the nanocrystals and the Y-poor domains, giving rise to the continuous decrease in the scattering contrast with increasing energy.[12,14]

When a crystal of differing composition nucleates in an otherwise homogeneous matrix, one expects the growth of the crystal to be limited by chemical diffusion. Such diffusion-limited growth is expected to follow a growth law of the form $R \propto t^{1/2}$, where R is the average crystal radius and t is the annealing time.[25] The crystal is surrounded by a compositionally altered zone. The crystal growth rate may fall below that predicted by the above law if (1) the crystals nucleate and grow into a compositionally inhomogeneous matrix where they grow ''against'' the composition gradient, or (2) multiple crystals nucleate in a homogeneous matrix and the compositionally altered zones surrounding neighboring crystals mutually impinge. Both mechanisms lead to a rapid falloff in the expected growth rate. A log-log plot of the apparent radius of gyration R_g (which is a measure of the crystal size) as a function of annealing time reveals a growth rate slightly slower than the $t^{1/2}$ dependence, particularly after long annealing times (Fig. 6). The apparent limiting value of R_g of 95 Å can be attributed mainly to one of the two mechanisms mentioned above. In case (1), the bcc nanocrystals nucleate in an already phase-separated liquid within a phase-separated domain of favorable composition. Subsequent growth is limited by the size of those decomposed areas. Growth into a neighboring phase-separated domain is suppressed due to the unfavorable composition. In case (2), the initial matrix is homogeneous and crystal growth is limited by impingement of the compositionally altered zones around neighboring crystals. For case (2), the crystalline phase comes to chemical equilibrium with a matrix of differing but ultimately uniform composition, i.e., one achieves two-phase chemical equilibrium.

Based on our DSC and (A)SAXS results and the high-resolution TEM studies previously carried out in the present system[9] we suppose that a phase separation of the undercooled liquid during preparation from the liquid precedes the nucleation of the bcc nanocrystals. The phase-separated domains are MgLi rich and Y poor and MgLi poor and Y rich, respectively. Copper is not involved in the phase separation. The nanocrystals of the bcc-Mg_7Li_3 phase nucleate within the Y-poor phase-separated domains. The upper limit for R_g of the nanocrystals of 95 Å is close to the estimated R_g of the phase-separated domains in the as-prepared sample. These facts favor case (1) as the main mechanism of crystallization in $Mg_{62}Cu_{25}Y_{10}Li_3$. Another limiting factor for the size of the nanocrystals could be the depletion of Li, which is the component with the smallest atomic fraction in the alloy. The nanocrystallization is not polymorphic; the ASAXS data indicate that during crystallization a Cu composition gradient between nanocrystals and matrix develops, most probably Cu depletes in the bcc-Mg_7Li_3 nanocrystals.

IV. SUMMARY

Phase separation is observed in the as-prepared splat-quenched $Mg_{62}Cu_{25}Y_{10}Li_3$ amorphous alloy and the domain interfaces seem to be surface fractals. Upon isothermal annealing at 135 °C for 30 min, nanocrystals of the bcc-Mg_7Li_3 phase are formed with an initial apparent R_g of 58 Å in MgLi-rich phase-separated domains. The crystals grow with annealing time, and reach a maximum R_g of 95 Å. Further growth of these crystals is constrained by the size of the domains and the depletion of Li. The interfaces of the nanocrystals in the early stages of annealing are rough and become sharper with increasing annealing when the average crystal size reaches a maximum R_g of 95 Å. The ASAXS investigation of a sample annealed for 120 min at 135 °C indicates that during crystallization a Cu composition gradient evolves between the bcc nanocrystals and the MgLi-rich domains.

ACKNOWLEDGMENTS

This work has benefited from the use of the beamline BL 4-2 at the Stanford Synchrotron Radiation Laboratory (SSRL), which is jointly funded by NIH and DOE. The effort of P.T. was supported by the U.S. Department of Energy, Office of Basic Energy Sciences, Division of Materials Science, under contract No. W-31-109-ENG-38 to the University of Chicago. The financial support from the DOE (Grant No. DEFG-03-86ER-45242), from the Deutsche Forschungsgemeinschaft via Sonderforschungsbereich 345 and from NATO grant CRG.961201 is gratefully acknowledged. We thank Dr. Hiro Tsuruta, SSRL, for his assistance in the SAXS measurements. P.T. is indebted to Dr. Greg Beaucage, University of Cincinnati, for his generosity in sharing the SAXS analysis package developed on IGOR Pro platform as well as for his time.

*Present address: SAP Technology, Inc., Palo Alto, CA 94304.

†Author to whom correspondence should be addressed.

[1] W. L. Johnson, Curr. Opin. Solid State Mater. Sci. **1**, 383 (1996).

[2] A. H. Okumura, A. Inoue, and T. Masumoto, Acta Metall. Mater. **41**, 915 (1993).

[3] K. Sugiyama, A. H. Shinohara, Y. Waseda, S. Chen, and A. Inoue, Mater. Trans., JIM **35**, 481 (1994).

[4] R. Busch, S. Schneider, A. Peker, and W. L. Johnson, Appl. Phys. Lett. **67**, 1544 (1995).

[5] S. Schneider, U. Geyer, P. Thiyagarajan, R. Busch, R. Schulz, K. Samwer, and W. L. Johnson, Mater. Sci. Forum **59**, 225 (1996).

[6] S. Schneider, P. Thiyagarajan, and W. L. Johnson, Appl. Phys. Lett. **68**, 493 (1996).

[7] A. Inoue, A. Kato, T. Zhang, S. G. Kim, and T. Masumoto, Mater. Trans., JIM **32**, 609 (1991).

[8] A. Inoue, T. Nakamura, N. Nishiyama, and T. Masumoto, Mater. Trans., JIM **33**, 937 (1992).

[9] W. Liu and W. L. Johnson, J. Mater. Res. **11**, 2388 (1996).

[10] W. Klement, Jr., R. H. Willens, and P. Duwez, Nature (London) **187**, 869 (1960).

[11] S. Wakatsuki, K. O. Hodgson, D. Eliezer, M. Rice, S. Hubbard, N. Gills, S. Doniach, and U. Spann, Rev. Sci. Instrum. **63**, 1736 (1992).

[12] H. B. Stuhrmann, Q. Rev. Biophys. **14**, 433 (1981).

[13] J. E. Epperson and P. Thiyagarajan, J. Appl. Crystallogr. **21**, 652 (1988).

[14] P. Thiyagarajan, K. A. Carrado, S. R. Wasserman, K. Song, and R. E. Winans, Rev. Sci. Instrum. **67**, 1 (1996).

[15] The glass transition and crystallization temperatures usually depend on the heating rates. This is demonstrated for the $Mg_{65}Cu_{25}Y_{10}$ alloy in R. Busch, W. Liu, and W. L. Johnson, J. Appl. Phys. **83**, 4134 (1998).

[16] A. Guinier and G. Fournet, *Small-Angle Scattering of X-Rays* (Wiley, New York, 1955), pp. 126–160.

[17] G. Porod, in *Small Angle X-Ray Scattering*, edited by O. Glatter and O. Kratky (Academic, New York, 1982), Chap. 2.

[18] Wavemetrics, Inc., Lake Oswego, OR 97035.

[19] G. Beaucage, J. Appl. Crystallogr. **28**, 717 (1995).

[20] B. B. Mandelbrot, *The Fractal Geometry of Nature* (Freeman, San Francisco, 1983).

[21] H. D. Bale and P. W. Schmidt, Phys. Rev. Lett. **53**, 596 (1984).

[22] D. W. Schaefer, J. E. Martin, P. Wiltzius, and D. S. Cannell, Phys. Rev. Lett. **52**, 2371 (1984).

[23] T. Freltoft, J. K. Kjems, and S. K. Sinha, Phys. Rev. B **33**, 269 (1986).

[24] B. Jacrot and G. Zaccai, Biopolymers **20**, 2413 (1981).

[25] F. E. Luborsky, *Amorphous Metallic Alloys* (Butterworths, London, 1983), pp. 156–159.